

EVIDENCE OF A MISALIGNED SECONDARY BAR IN THE LARGE MAGELLANIC CLOUD

ANNAPURNI SUBRAMANIAM

Indian Institute of Astrophysics, Koramangala II Block, Sarjapur Road, Bangalore 560034, India

Received 2003 November 17; accepted 2004 February 2; published 2004 February 26

ABSTRACT

Evidence of a misaligned secondary bar, within the primary bar of the Large Magellanic Cloud (LMC), is presented. The density distribution and the dereddened mean magnitudes (I_0) of the red clump stars in the bar obtained from the Optical Gravitational Lensing Experiment II data are used for this study. The bar region that predominantly showed a wavy pattern in the line of sight in a recent paper by Subramaniam was located. These points in the X - Z plane delineate an S-shaped pattern, clearly indicating a misaligned bar. This feature is statistically significant and does not depend on the considered value of I_0 for the LMC center. The rest of the bar region was not found to show the warp or the wavy pattern. The secondary bar is found to be considerably elongated in the Z -direction, with an inclination of $66^\circ 5' \pm 0^\circ 9'$, whereas the undisturbed part of the primary bar is found to have an inclination of $15^\circ 1' \pm 2^\circ 7'$, such that the eastern sides are closer to us with respect to the western sides of both the bars. The P.A._{maj} of the secondary bar is found to be $108^\circ 4' \pm 7^\circ 3'$. The streaming motions found in the H I velocity map close to the LMC center could be caused by the secondary bar. The recent star formation and the gas distribution in LMC could be driven by the misaligned secondary bar.

Subject headings: galaxies: stellar content — galaxies: structure — Magellanic Clouds

1. INTRODUCTION

The off-centered stellar bar is one of the most striking features of the Large Magellanic Cloud (LMC). On the other hand, it is one of the least studied and understood features of the LMC. The near-IR star count maps presented by van der Marel (2001) found the bar to be a smooth structure, even though a *peak* in the ellipticity and change in position angle (P.A.) were found within the central 2° . Recently Subramaniam (2003) studied the relative distance within the LMC bar using the dereddened mean magnitudes of red clump stars; she found that the bar is warped and also found structures in the bar. In an attempt to find out the possible reason for these structures, we came across evidence of a possible existence of a secondary bar within the LMC bar. Bars are a common phenomenon in late-type spirals and Magellanic irregulars (de Vaucouleurs & Freeman 1973). Recent studies find that the secondary bars within large-scale bars are also common, occurring in about a third of barred galaxies (Jungwiert, Combes, & Axon 1997; Laine et al. 2002; Erwin & Sparke 2002; Erwin 2004).

The evidence of a possible existence of the secondary bar has been found in the literature. Some of the significant references are discussed below. In the R -band isophotes of de Vaucouleurs (1957), the first contour shows the bar; two contours immediately next to this suggest a turn in the top left and bottom right corners of the bar. This is the first evidence for the twist of the isophotes within the central region of the LMC bar. The isophotes are based on R -band photometry, and hence contribution from the old stars dominates. Such an isophotal twist would manifest as change in the P.A. of the major axis in the central region, change in ellipticity, and a possible counterrotation in the inner regions of the LMC. The evidence of the change in P.A. and ellipticity near the LMC center can be found in the literature. Some references are indicated below. Figure 3 in van der Marel (2001) shows the change in P.A. and ellipticity; Figure 6 in van der Marel et al. (2002) shows change in P.A. for the carbon stars; and Figure 5 in Kim et al. (1998) shows the change in P.A. for H I. The presence of the above two features found in the central region of NGC 2950 is taken as the photometric signature of a misaligned secondary

bar (Corsini, Debattista, & Aguerri 2003). Recent investigations of double-barred galaxies (Erwin 2004; Jungwiert et al. 1997) indicate that in general, the radial plot of the ellipticity reflects a double peak corresponding to both the bars in the galaxy. In the case of LMC, Figure 3 in van der Marel (2001) indicates the first peak, $\epsilon_{\max} \sim 0.7$ at $r \sim 1^\circ$. This is well within the primary bar, which extends to more than 2° radius. The second peak appears after a radial distance of 2° , although it is not very prominent. The corresponding $\epsilon_{\max} \sim 0.57$. Evidence of negative rotational velocity with respect to the center of LMC is noted in a number of cases. The study of CH stars by Hartwick & Cowley (1988) found that some stars have negative galactocentric velocity. Similar cases are also found in the case of planetary nebulae and old star clusters. Hartwick & Cowley (1988) state that these stars may be related in some way to the bar of the LMC. Recent studies of carbon star kinematics by van der Marel et al. (2002) find that within the central 1° , the mean rotational velocity is $\sim -28 \text{ km s}^{-1}$. Thus all the above observations point to the possible existence of a misaligned secondary bar. All these are features observed in the projected two dimensions, and no information is available on its possible appearance in the line of sight.

In the present study, we explore the presence of the secondary bar within the LMC bar in the projected two-dimensional X - Y plane as well as in the X - Z plane. We use the red clump stars in the second Optical Gravitational Lensing Experiment (OGLE II) catalog as the probe for this study. The density of red clump stars in the bar region is used to study the projected pattern. The relative distance estimates in the LMC bar based on the dereddened mean magnitudes of red clump stars, presented in Subramaniam (2003), are used to study the pattern in the line of sight.

2. BAR IN THE PROJECTED TWO DIMENSIONS

The OGLE II survey (Udalski et al. 2000) consists of photometric data of 7 million stars in B , V , and I passbands in the central 5.7 deg^2 of LMC. The observed bar region was divided into 1344 sections ($3.56 \times 3.56 \text{ arcmin}^2$). The red clump stars were identified using an I versus $(V-I)$ color-magnitude dia-

gram, and on an average, 2000 red clump stars were identified per region. The data suffer from the incompleteness problem due to crowding effects, and the incompleteness in the data in I and V passbands is tabulated in Udalski et al. (2000). After correcting for the data incompleteness, the total number of red clump stars in each area bin and the number density of the red clump stars per square degree were estimated. The center of the LMC is taken to be R.A. = $05^{\text{h}}19^{\text{m}}38^{\text{s}}$, decl. = $-69^{\circ}27'5''$ (J2000.0; de Vaucouleurs & Freeman 1973). The location of each area bin is converted to the linear X, Y coordinates using the convention in van der Marel & Cioni (2001), and these data are used for the following analysis.

The two-dimensional distribution of the red clump star density on the X - Y plane is shown in the top left panel of Figure 1. The figure shows maximum density near the center that decreases radially outward. The main feature is the elongation of the central density to the eastern side, and this elongation is then carried outward as ellipses. This is found to be the origin of the elliptical pattern found in the bar. The major axis of the ellipse is found to turn very clearly in the east side. This is indicative of isophotal twist. The maximum density at each radial point is estimated, and its variation with respect to radius is shown in the bottom panels of Figure 1. The profiles are different for the east and west sides of the bar. The profile on the east side is characterized by a shallower slope up to $0^{\circ}6$ and a steeper slope up to $1^{\circ}9$. Beyond this, the profile is found to be very flat. The other features that could also be noted are the likelihood of a rise close to the center, at $0^{\circ}6$ and $1^{\circ}3$. The rise of the profile near the center could indicate a very compact bulge, which could not be confirmed here. The points are connected using a smoothing function that takes the average of the two neighboring points. The profile for the east side is very similar to the magnitude variation along the major axis of a double-barred galaxy (e.g., NGC 1291; de Vaucouleurs 1975, Fig. 10). The prominent peak corresponding to the bulge is missing here, with the rest of the profile looking very similar. NGC 1291 is considered a prototype of double-barred galaxies (Friedli & Martinet 1993). The west side profile is different, with the slope similar to that seen between $0^{\circ}6$ and $1^{\circ}9$ for the eastern side and a rise in the profile at $1^{\circ}3$. The variation of the P.A. of the major axis as a function of radial distance is shown in the top right panel of Figure 1. Considerable change in the P.A. with radial distance can be noted. Turnover of the P.A. at radial distances of $0^{\circ}8$, $1^{\circ}4$, and $1^{\circ}9$ on the eastern side and $1^{\circ}3$ on the western side could be noted. Thus the turnovers of the P.A. are well correlated with the changes in the density profile. These variations thus suggest structures in the bar close to the center, with the possible existence of a secondary bar. The P.A. of the maximum density points is used to estimate the average P.A._{maj} of the bar. The average value of the P.A. of the major axis is found to be $123^{\circ}3 \pm 13^{\circ}3$ for the east and $105^{\circ}5 \pm 18^{\circ}1$ for the west side. The average P.A. of the primary bar is found to be $114^{\circ}0 \pm 22^{\circ}5$. This value tallies well with the earlier estimates of the P.A._{maj} for inner regions, which is dominated by the primary bar. The value of P.A._{maj} is $122^{\circ}5 \pm 8^{\circ}3$ (as estimated by van der Marel 2001) and $129^{\circ}9 \pm 6^{\circ}0$ (van der Marel et al. 2002).

3. THE LOCATION OF THE BAR IN THE Z-DIRECTION

The results presented in Subramaniam (2003) showed that there are structures in the bar indicating a wavy pattern running from the east to the west side of the bar. This was noted on and above the warp, where the western end as well as the

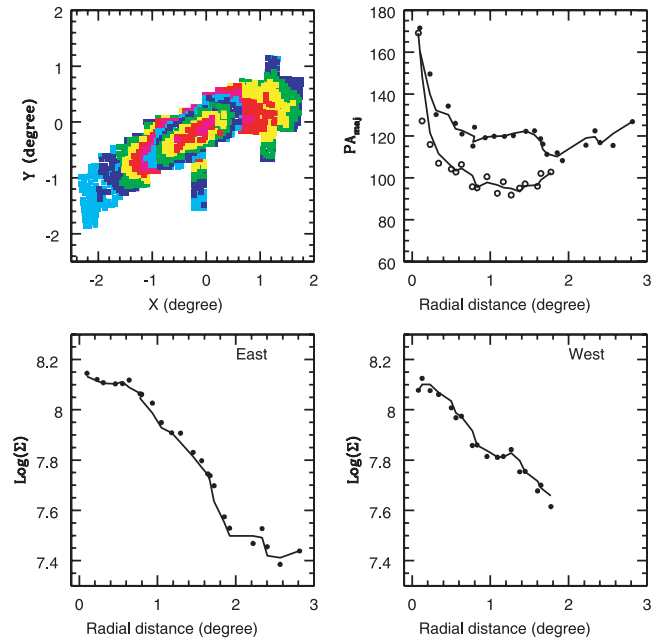


FIG. 1.—Density distribution of the red clump stars is presented in the top left panel. The central region indicated in magenta has density more than 1.3×10^8 stars deg^2 . The color code used is such that the density decreases from magenta to cyan, with density intervals of 0.1×10^8 stars deg^2 . The second appearance of magenta has density between 0.8×10^8 and 0.7×10^8 , and the points indicated in cyan at the east end of the bar have density less than 0.3×10^8 . The variation of P.A. of the major axis with radial distance is shown for the east side (filled circles) and west side (open circles) of the bar in the top right panel. A smoothing function of width 2 is used to connect the points. The radial variation of the maximum value of the red clump density is shown for the east (left) and west (right) sides of the bar in the bottom panel. The points are connected using a smoothing function, which takes the average of two adjoining points.

eastern end were found to be closer to us with respect to the LMC center. The data presented in Subramaniam (2003) were transferred to the X - Y plane using the assumed LMC center. The points at which the bar was found to be located away from us (i.e., at R.A. $\sim 84^{\circ}$; decl. $\sim -70^{\circ}$ and LMC center and R.A. $\sim 76^{\circ}$; decl. $\sim -69^{\circ}$) are found to lie in one line. The P.A. of the axis coinciding with this line is $109^{\circ} \pm 3^{\circ}$.

Figure 3 of Subramaniam (2003) was converted into the X - Z plane, where the Z -values were obtained by converting the I_0 -values. The I_0 -value at the location of the LMC center, 18.20 ± 0.01 mag, was taken as $Z = 0$. The difference in the value of I_0 between any location and the LMC center is estimated, and then this value is multiplied by 25 kpc, since a shift in 0.1 mag in I corresponds to a shift of 2.5 kpc. Since Z is in units of kpc, we convert X also in units of kpc using the relation $1^{\circ} = 0.89$ kpc. The magnitude errors in the data points were also converted to errors in distance. As the bar is seen to be perturbed along the P.A., $109^{\circ}0$, the locations between $\pm 12^{\circ}0$ of this P.A. were chosen. All the points within a radius of $0^{\circ}4$ were also included, as the above selection results in severe undersampling of data points near the center. These points are shown in the top panel of Figure 2, where the left panel shows the X - Y plane and the right panel shows the X - Z plane. In the X - Y plane, the points with $Z > 0$ are shown as filled circles. In the X - Z plane, the dotted lines correspond to the location where a change in radial density profile was noted in Figure 1, at radial distances of $1^{\circ}9$ and $1^{\circ}3$ in the east and west sides, respectively. Within these two lines, a well-defined

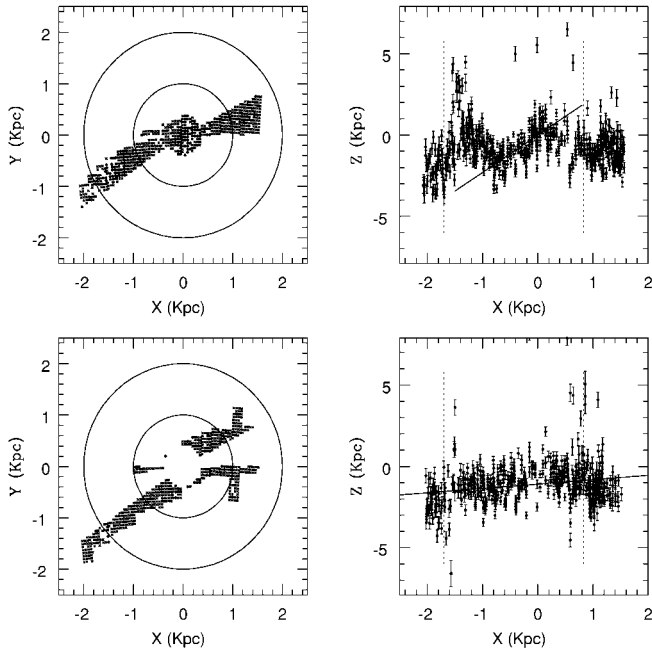


FIG. 2.—Location of the primary bar within $P.A. = 110^\circ 0 \pm 12^\circ 0$ is shown in the X - Y and X - Z planes in the top panel. The location of the rest of the bar in the X - Y and X - Z planes is shown in the bottom panel. The circles in the left panels are drawn at $1^\circ 0$ and $2^\circ 0$ radii. The filled circles in the left panels indicate points that have $Z > 0.0$. The dotted lines shown in the right panels correspond to locations showing change in density profiles. The errors in the data points are obtained from Subramaniam (2003), where the ΔI_0 -values are converted to kiloparsecs as explained in the text.

S-shaped pattern can be noted. The variations seen in the feature are statistically significant, as indicated by the error bars. The maximum random error as estimated by Subramaniam (2003) was 0.02 mag in I_0 , and this corresponds to 500 pc as per the above conversion. The variation as shown in the figure corresponds to more than 1.5 kpc, which has 3σ significance with respect to the maximum random error. The feature found in the X - Z plane is not dependent on the I_0 -value chosen for the center. The same pattern is observed when the I_0 magnitudes are plotted against the X coordinate. Hence this feature does not depend on the value of I_0 considered for the conversion to the Z -axis.

The S-shaped pattern consists of the central bar inclined in the line of sight with trailing pattern on both ends. This feature is considered the misaligned secondary bar. The eastern end of the secondary bar is seen to be closer with respect to the western end. Thus a part of the primary bar is disturbed because of the presence of the secondary bar. On both ends of the secondary bar, the primary bar is sheared and has a depth of about 5 kpc. The nature of rotation of the bar could not be inferred from the present data, although the S-shaped pattern gives an impression of rotation in the counterclockwise direction. The central feature corresponding to the bar is fitted with a straight line as shown in the figure. The inclination of the bar is estimated from the slope and is found to be $66^\circ 5 \pm 0^\circ 9$. The value of the slope depends on the points chosen, and the above value was derived by obtaining the best value of correlation coefficient (0.78) for the least-squares fit. A deviation of $\pm 5^\circ 0$ for the slope is possible based on the choice of points. The P.A. of the major axis of the secondary bar is also estimated. The value was found to have a lot of scatter for points near the center. We estimated $P.A._{maj}$ to be $108^\circ 4 \pm$

$7^\circ 3$ for the bar outside the $0^\circ 4$ radius and $136^\circ 2 \pm 26^\circ 0$ for points within. The P.A. of the secondary is computed by taking only those data points that are used to fit the straight line. The P.A. of the secondary bar can be considered to be $108^\circ 4 \pm 7^\circ 3$, where the contribution from the central regions is not considered. The extent of the bar could not be estimated accurately, as the trailing patterns overlap. Also, the spiral pattern is clearly seen to be connected to the bar in the eastern side, but a clear connection is not seen in the western side. The upper limit to the length of the bar is estimated to be ~ 3.0 kpc. As indicated above, only a part of the bar is chosen to identify the secondary bar. This would mean that the rest of the bar should not show any variation in the line of sight. The bottom panel of Figure 2 shows the X - Y and X - Z plot of the rest of the bar. It is very clear from the X - Z plot that the rest of the bar does not show any wavy pattern or the warp. The data points are fitted with a straight line and are shown in the figure. The unperturbed part of the primary bar is thus slightly inclined, with a slope of 0.27 ± 0.05 , which corresponds to $15^\circ 1 \pm 2^\circ 7$. Thus the east end of the primary bar is closer to us than the west end.

4. RESULTS AND DISCUSSION

The possible existence of a secondary bar within the primary bar of LMC is explored here. The photometric signatures of the secondary bar are found plentifully in the literature, such as the twist of isophotes, change in the P.A. of the major axis, and ellipticity *peak* in the central regions. On the other hand, these signatures were never connected with the possible existence of a secondary bar. The motivation to look for a secondary bar came from the perturbations that were noted in the primary bar by Subramaniam (2003). The radial profile of the maximum density on the east side resembles the brightness profile of the double-barred galaxies along the major axis. The secondary bar is seen only on the east side. This indicates that the secondary bar is not symmetric with respect to the optical center. The secondary bar has disturbed only a part of the primary bar; hence, we are also able to estimate the parameters of the undisturbed primary bar. The undisturbed primary bar does not show any warp. Although the ellipticity of the bars could not be estimated here, the ellipticity estimations in the literature shows that the ellipticity of the secondary bar is $\epsilon_{max}^s \sim 0.7$, whereas that of the primary is $\epsilon_{max}^p \sim 0.57$. The catalog of double-barred galaxies presented by Erwin (2004) estimated that the average value of the ellipticity of the secondary bar in 49 galaxies is 0.3 , whereas the average value for the primary bar is 0.47 . The above values were found to be similar to the average ellipticity of the bars presented in Jungwiert et al. (1997) for 13 galaxies. Both the data also indicate that $\sim 85\%$ galaxies show higher ellipticity value for the primary bar when compared to that of the secondary bar. On the other hand, LMC shows higher ellipticity for the secondary bar, which is seen in $\sim 15\%$ of the double-barred galaxies. It can be seen that the difference between the P.A.'s of the primary and the secondary bar is very small. The $\Delta P.A. = 8^\circ 0 \pm 23^\circ 0$, which is very small or close to zero within errors. LMC belongs to the group of 6% of double-barred galaxies, which show very small value for $\Delta P.A.$ (Erwin 2004). The bars are not aligned in the Z -direction, as indicated by the inclination values of $66^\circ 5 \pm 0^\circ 9$ and $15^\circ 1 \pm 2^\circ 7$ for the primary and the secondary bars, respectively. The main signature that reveals the central structure as a secondary bar is the misalignment in the Z -direction, more than the ellipticity and isophotal signatures. This is the reason

that the central structure is claimed to be a misaligned secondary bar. The spiral-like patterns on the ends of the secondary bar could suggest a possible counterclockwise rotation in the X - Z plane. The presence of a misaligned secondary bar could give rise to kinematic signatures near the central regions. The negative rotational velocity noted in the central regions could be due to the secondary bar. The misalignment could also produce noncircular motions. As the feature in the X - Z plane does not show any ring, either the secondary bar has a slow pattern speed or it is recently formed. More studies are required to understand this newly found feature in the LMC.

The signatures of the secondary bar could be traced in H I observations. The velocity field of the H I, as shown in Figure 4 of Kim et al. (1998), indicates a steep velocity gradient just to the north of the center of the bar. This is considered the dynamical evidence of large-scale streaming motions. Such a steep velocity gradient was also noted by Luks & Rohlfs (1992). It is quite possible that the secondary bar is responsible for the streaming motions. The elongation of the secondary bar in the Z -direction could give rise to a steep velocity gradient. The H I observations by Kim et al. (1998) show a two-armed spiral pattern in their Figure 2. Similar spiral arm features were also

observed by Staveley-Smith et al. (2003, Fig. 2), and they remark that the two arms are connected by H I but not in a structure that looks like the bar, as the position of the optical bar is different. The secondary bar could be the feature that is connecting the two spiral arms. The H I observation of Rohlfs et al. (1984) finds clear indications of noncircular velocity near the center. In Figure 5 of Rohlfs et al. (1984) and Figure 8 of Luks & Rohlfs (1992), the velocity map of H I clearly indicates a lower velocity to the south of the thickly populated isovelocity contours near the LMC center and a higher velocity to the north. This suggests a rotation in the sense that the southern part is moving toward us and the northern part is moving away with respect to the center. This corresponds to a shift in the X - Z plane, in good agreement with the shift of the secondary bar, if the secondary bar has a counterclockwise rotation. Thus the secondary bar of the LMC could be the missing link between the stellar and the gas distribution in the LMC. The recent star formation and the gas distribution in the LMC could be driven by this misaligned secondary bar.

I thank T. P. Prabhu and Daniela Vergani for helpful discussions.

REFERENCES

- Corsini, E. M., Debattista, V. P., & Aguerrri, J. A. L. 2003, *ApJ*, 599, L29
 de Vaucouleurs, G. 1957, *AJ*, 62, 69
 ———. 1975, *ApJS*, 29, 193
 de Vaucouleurs, G., & Freeman, K. C. 1973, *Vistas Astron.*, 14, 163
 Erwin, P. 2004, *A&A*, in press (astro-ph/0310806)
 Erwin, P., & Sparke, L. S. 2002, *AJ*, 124, 65
 Friedli, D., & Martinet, L. 1993, *A&A*, 277, 27
 Hartwick, F. D. A., & Cowley, A. P. 1988, *ApJ*, 334, 135
 Jungwiert, B., Combes, F., & Axon, D. J. 1997, *A&AS*, 125, 479
 Kim, S., Staveley-Smith, L., Dopita, M. A., Freeman, K. C., Sault, R. J., Kesteven, M. J., & McConnell, D. 1998, *ApJ*, 503, 674
 Laine, S., Shlosman, I., Knapen, J. H., & Peletier, R. F. 2002, *ApJ*, 567, 97
 Luks, Th., & Rohlfs, K. 1992, *A&A*, 263, 41
 Rohlfs, K., Kreitschmann, J., Siegman, B. C., & Feitzinger, J. V. 1984, *A&A*, 137, 343
 Staveley-Smith, L., Kim, S., Calabretta, M. R., Haynes, R. F., & Kesteven, M. J. 2003, *MNRAS*, 339, 87
 Subramaniam, A. 2003, *ApJ*, 598, L19
 Udalski, A., Szymański, M., Kubiak, M., Pietrzyński, G., Soszyński, I., Woźniak, P., & Żebruń, K. 2000, *Acta Astron.*, 50, 307
 van der Marel, R. P. 2001, *AJ*, 122, 1827
 van der Marel, R. P., Alves, D. R., Hardy, E., & Suntzeff, N. B. 2002, *AJ*, 124, 2639
 van der Marel, R. P., & Cioni, M.-R. 2001, *AJ*, 122, 1807